Spectral–Spatial Classification and Shape Features for Urban Road Centerline Extraction

Wenzhong Shi, Zelang Miao, Qunming Wang, and Hua Zhang

***Abstract*—This letter presents a two-step method for urban main road extraction from high-resolution remotely sensed imagery by integrating spectral–spatial classification and shape features. In the first step, spectral–spatial classification segments the imagery into two classes, i.e., the *road* class and the *nonroad* class, using path openings and closings. The local homogeneity of the gray values obtained by local Geary's C is then fused with the *road* class. In the second step, the *road* class is refined by using shape features. The experimental results indicated that the proposed method was able to achieve a comparatively good performance in urban main road extraction.**

***Index Terms*—High-resolution remotely sensed imagery, local Geary's C, main road extraction, path openings and closings, shape features, spectral–spatial classification.**

I. Introduction

ROAD information is vital in the management of many aspects of daily life such as urban design, navigation, and image registration. With the aid of computer technology, road extraction from remotely sensed imagery is an economic and effective way to acquire road information. Over the past decades, various road extraction algorithms have been proposed [1]. Many methods are region based [2]–[6] which extract initial road networks based on classification. As such, region-based road extraction methods depend on the accurate classification results. Satisfactory classification results, however, are difficult to obtain because most classification methods are based only on spectral information and do not consider the spatial features of the image. To enhance classification accuracy, spectral–spatial classification [7] which uses both spectral and spatial information has been proposed. In this field, local spatial statistics [8], [9] which measure local autocorrelation have been used to describe spatial information. Mathematical morphology (MM) is also one of commonly used methods to produce image spatial structures [10]–[12]. However, classical MM depends on a fixed shape structuring element (SE). Consequently, this method is not sufficiently flexible to simultaneously detect curved and rectilinear structures. Other spectral–spatial classification methods can be found in the paper written by Plaza *et al.* [7]. Another approach to incorporate spatial information consists in the use of the road's shape features [4], [13]–[15]. Although the integration of shape features shows a good performance in road extraction, it is difficult to obtain universal shape feature extraction methods for all situations [13], and further study is necessary.

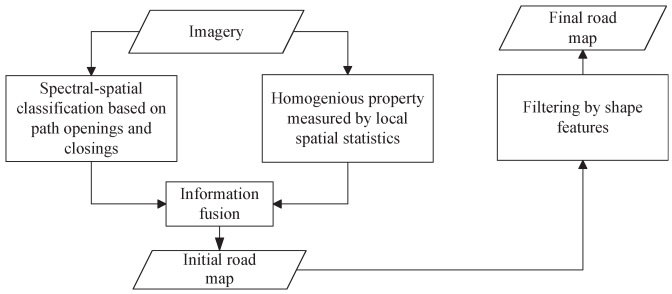

Fig. 1. Flowchart of the proposed method.

In this letter, a new method for urban main road extraction from high-resolution remotely sensed imagery is proposed. This method integrates spectral–spatial classification and shape features and consists of two steps. First, path openings and closings are used to produce morphological profiles (MPs) for spectral–spatial classification, and the imagery is classified into two categories, i.e., the *road* class and the *nonroad* class. The local Geary's C is then used to measure the local homogeneity of the gray values. After that, classification and the local homogeneity results are combined by information fusion rule. Second, the *road* class is filtered by shape features to remove misclassified roads.

The remainder of this letter is organized as follows. In Section II, the new method is presented. Experimental results are reported in Section III. Conclusions are drawn in Section IV.

II. Methodology

As indicated earlier, the focus of this letter is urban "main road" extraction from high-resolution remotely sensed imagery. The definition of "main road" depends on the road width. Roads whose width is greater than a threshold are considered as "main roads." Fig. 1 gives a summary of the proposed method.

Manuscript received March 28, 2013; revised June 8, 2013, August 12, 2013, and August 15, 2013; accepted August 16, 2013. Date of publication September 9, 2013; date of current version December 2, 2013. This work was supported in part by the National Natural Science Foundation of China under Grants 41201451 and 40901214, by the Ministry of Science and Technology of China under Projects 2012BAJ15B04 and 2012AA12A305, by the Research Grants Council, Hong Kong, under Grant PolyU 5249/12E, and by The Hong Kong Polytechnic University under Projects 1-ZVBA, G-U753, G-YK75, and G-YJ75.

W. Shi and Q. Wang are with the Joint Research Laboratory on Spatial Information, The Hong Kong Polytechnic University–Wuhan University, 430079, China.

Z. Miao is with the Department of Land Surveying and Geo-Informatics, The Hong Kong Polytechnic University, Kowloon, Hong Kong, and also with the School of Environmental Science and Spatial Informatics, China University of Mining and Technology, Xuzhou 221116, China (e-mail: cumtzlmiao@gmail.com).

H. Zhang is with the School of Environmental Science and Spatial Informatics, China University of Mining and Technology, Xuzhou 221116, China.

Color versions of one or more of the figures in this paper are available online at http://ieeexplore.ieee.org.

Digital Object Identifier 10.1109/LGRS.2013.2279034

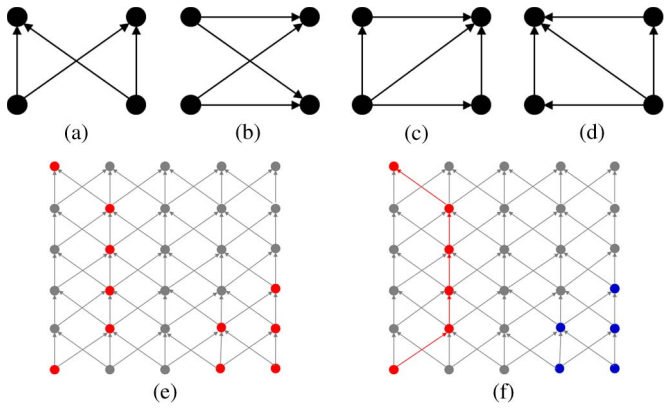

Fig. 2. (a)–(d) Four different adjacency relationships. (e) Original data points are shown in red, and the adjacency is shown in gray. (f) The result of path opening with $L_{\min} = 6$. The retained and discarded pixels are shown in red and blue, respectively.

A. Spectral–Spatial Classification

The purpose of step A is to classify the imagery into *road* and *nonroad* classes using spectral–spatial classification based on path openings and closings. The path opening and closing method was first proposed by Buckley and Talbot [16], and the theoretical foundation was given by Heijmans *et al.* [17]. The main idea of path openings and closings is to replace classical MM's SEs by a family of nonstraight line segments with flexible length $L_{\min}$. A path opening of $L_{\min}$ is equivalent to the supremum of all openings with SEs composed of $L_{\min}$ connected pixels that are arranged according to a specific adjacency relationship [18]. Fig. 2(a) and (d) shows four different adjacency relationships, and Fig. 2(e) and (f) presents an example of path openings. To avoid adjacency relationship selection, the supremum of openings on these four adjacencies and the infimum for closings are selected [18]. Detailed information about path openings and closings is presented in [16]–[18].

The spectral–spatial classification is implemented by the following two steps.

1) Generate MPs by applying path openings and closings. MPs [11] are a composition of morphological processing with an increasing size of the SE. These elements contain the information about size and shape of objects in the image [11]. The MPs at the pixel x_{ij} of the image I are computed as

$$\mathrm{MP}(x_{ij}) = \{\mathrm{PathClosing}_{L\min=n}(x_{ij}), \ldots, I(x_{ij}) \ldots, \mathrm{PathOpening}_{L\min=n}(x_{ij})\}. \quad (1)$$

2) Implement classification with support vector machine (SVM) [19], taking MPs as input features. In this letter, Gaussian kernel is selected, and the parameters C and γ are determined by fivefold cross-validation.

B. Homogeneous Property Measurement

The goal of step B is to measure the local homogeneity of the gray values using local spatial statistics [20]. The local spatial statistics have three commonly used indices: 1) Getis–Ord G_i; 2) local Moran's I; and 3) local Geary's C. Getis–Ord G_i detects hot spots well, local Moran's I identifies pixel clustering, and local Geary's C detects edge areas. Since the purpose of homogeneous property measurement is to distinguish homogeneous areas from edges, local Geary's C is selected to characterize the local homogeneity of the gray values.

The local Geary's C is defined as

$$c(x_{ij}) = \frac{w^2}{\sum_a \left(I(x_a) - \bar{I}_w(x_{ij})\right)} \sum_a \sum_b w_{ab}(d) \times [I(x_a) - I(x_b)]^2 \quad (2)$$

where w is the window size, x_a and x_b denote two pixels in the window, $I(x_a)$ and $I(x_b)$ are their corresponding gray values, $\bar{I}_w(x_{ij})$ is the mean of all pixels' gray values in the window, d is the distance between x_a and x_b, and w_{ab} is the weight at distance d so that $w_{ab}(d) = 1$ if point x_a is within distance d from point x_b or $w_{ab}(d) = 0$ if otherwise. The window size of local Geary's C is determined by experiment results. Small homogeneous regions cannot be correctly measured by local Geary's C with a large window size (i.e., 6×6 pixels). Therefore, the window size is set to 2×2 pixels in this letter.

Here, an approach to compute local Geary's C index from the B-band multispectral remotely sensed imagery is presented. Specifically, the local Geary's C indices of all bands are computed and then averaged

$$\bar{c}(x_{ij}) = \frac{1}{B} \sum_{\lambda=1}^{B} c_\lambda(x_{ij}) \quad (3)$$

where $c_\lambda(x_{ij})$ is the local Geary's C of band λ at the pixel $x_{ij}, \lambda = 1, 2, \ldots, B$.

The homogeneous regions have low values of local Geary's C, while edge pixels have large values. Therefore, homogeneous regions can be extracted by thresholding on the local Geary's C map.

C. Information Fusion

It is difficult to completely separate roads from other man-made objects based only on classification [4] due to the urban image complexity. A solution is to fuse different road characteristics. In this study, the classification result and the local homogeneity of the gray values are combined by an information fusion scheme to improve the initial road map accuracy. The information fusion scheme is defined as

$$x_{ij} = \begin{cases} \text{road, if } x_{ij} \text{ is assigned to class } road \\ \quad \text{in step A and } \bar{c}(x_{ij}) \le T_c \\ \text{nonroad, otherwise.} \end{cases} \quad (4)$$

The T_c is defined as

$$T_c = \mathrm{median}(Q) \quad (5)$$

where $Q = \{\bar{c}(x_{ij}) | x_{ij} \text{ is assigned to class } road \text{ in step A}\}$.

D. Shape Features

After information fusion, some misclassified roads are removed. However, information fusion cannot discard misclassified roads completely. To further discard misclassified roads, road shape features are explored. These features are measured by the following: 1) area; 2) linear feature index (LFI); and

3) average length between two junctions (ALJ), which are introduced as follows.

1) *Area*: A road is commonly a continuous feature with a relatively larger area than other man-made features. Hence, segments with small area values can be viewed as *nonroad* class and removed.
2) *LFI*: Roads are generally narrower and longer than other artificial objects. This characteristic is described by LFI which is computed as follows.
   a) Using connected component analysis to divide pixels into connected components and extracting the centerline for each component by the method proposed by Uitert and Bitter [21]. The component is then converted to a rectangle which satisfies

$$\begin{aligned} &LW = n_p \\ &\text{s. t. } L = \text{length of centerline of component} \\ &\quad n_p = \text{area of the component} \end{aligned} \tag{6}$$

   where L and W are the length and width of the new rectangle and n_p is the component area.
   b) LFI is calculated by

$$\text{LFI} = \frac{L}{W} = \frac{L}{n_p/L} = \frac{L^2}{n_p}. \tag{7}$$

   The road should have a large LFI value; thus, segments with small LFI values are removed.
3) *ALJ*: ALJ is calculated by the following three steps.
   a) Extraction of the centerline of each component.
   b) Calculation of the length and junction number of the centerline. Any pixel that has more than two neighboring pixels is defined as the junction. In this letter, the junction is detected using the mathematical morphological method [22].
   c) ALJ is calculated by

$$\text{ALJ} = L/(n_J + 1) \tag{8}$$

   where n_J is the junction number and $n_J + 1$ is to prevent the expression to have a zero denominator.

   In the real world, the distance between two road junctions should not be too short. Therefore, segments with small ALJ values are removed. Above all, segments which satisfy (9) will be judged as road

$$S_{\text{Area}} \geq T_{\text{Area}} \text{ and } S_{\text{LFI}} \geq T_{\text{LFI}} \text{ and } S_{\text{ALJ}} \geq T_{\text{ALJ}} \tag{9}$$

   where S_{Area}, S_{LFI}, and S_{ALJ} denote the area, LFI, and ALJ values of the component, respectively. T_{Area}, T_{LFI}, and T_{ALJ} are the corresponding thresholds that are empirically determined.

III. Experimental Study

A. Tests on Spectral–Spatial Classification Methods

The proposed method is compared with some existing spectral–spatial classification methods in the literature. A part of a suburban satellite image in Xincheng District, Xuzhou City, was selected as the experimental data. The image was recorded by the multispectral spectrometer carried by the Ziyuan-3 satellite on August 11, 2012. The spatial resolution is 6 m per pixel, and the number of bands is four. In this letter, the road whose width is greater than four pixels is considered as the "main road." The reference road map is generated by hand drawing method. Fig. 3 shows the road extraction results of different spectral–spatial classification methods.

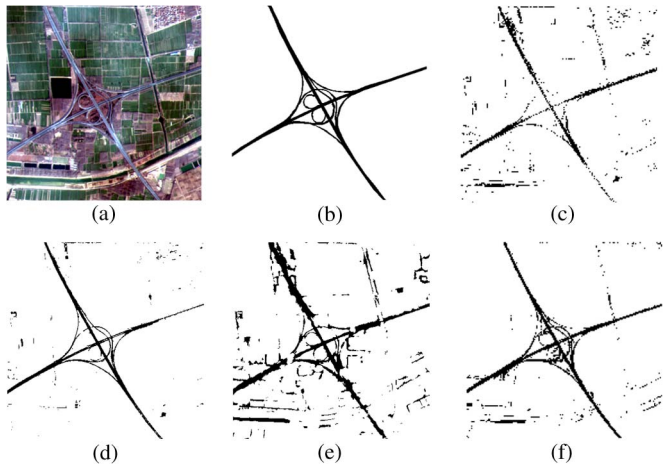

Fig. 3. (a) Original image. (b) Road reference map. (c) Road extraction result by pixelwise SVM. (d) Road extraction result by method of Tarabalka *et al.* [10]. (e) Road extraction result by method of Fauvel *et al.* [11]. (f) Road extraction result by the proposed method.

TABLE I
Comparison of Spectral–Spatial Classification Methods

Method	*Completeness*	*Correctness*	*Quality*
Pixel-wise SVM	0.55	0.56	0.39
Tarabalka's method	0.67	**0.84**	**0.60**
Fauvel's method	0.81	0.43	0.39
Proposed method	**0.81**	**0.68**	0.59

When quantifying the performance values, three accuracy measures proposed by Wiedemann *et al.* [23] were used to evaluate the proposed method: 1) Completeness $= \text{TP}/(\text{TP} + \text{FN})$; 2) Correctness $= \text{TP}/(\text{TP} + \text{FP})$; and 3) Quality $= \text{TP}/(\text{TP} + \text{FP} + \text{FN})$. TP, FN, and FP mean true positive, false negative, and false positive, respectively. TP is the length of matched extracted data within the buffer around the reference road data, FP is the length of unmatched extracted data, and FN is the length of referenced data which are not located within the buffer around the extracted data. The buffer width was set to 12 m in this study. The comparison results are presented in Table I.

As can be seen from Table I, incorporating spatial information into spectral–spatial classification methods significantly improves the road extraction accuracy. The highest road extraction accuracy is achieved when using spectral–spatial classifiers based on path openings and closings. More precisely, compared with those of the pixelwise SVM classification, the completeness and correctness of the proposed method are greater by 26% and 12%, respectively. Table I also indicates that the method by Tarabalka *et al.* and the proposed method achieved similar *quality* values. This is because the proposed method only implemented spectral–spatial classification without subsequent filtering based on shape features. The accuracy of the proposed method would be further improved by filtering using shape features.

B. Experiments

A subset of a Ziyuan-3 satellite image located in Jiuli District, Xuzhou City, was selected as the second study area. The

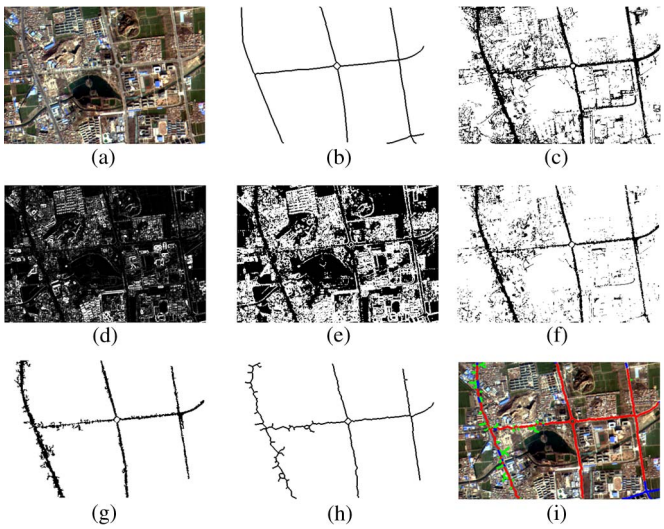

Fig. 4. (a) Image of the study area. (b) Hand-drawn road map. (c) SVM classification result. (d) Local Geary's C result. (e) Thresholding result of local Geary's C map. (f) Fusion result of (c) and (e). (g) Filtering result. (h) Road centerline extraction result. (i) Superposition result. True positives are shown in red, false positives in green, and false negatives in blue.

study area has a spatial dimension of 322×472 pixels. Fig. 4(a) shows the study area image. The road reference map obtained by visual interpretation methods is shown in Fig. 4(b).

First, MPs of all spectral bands were constructed by applying a series of path openings and closings with increasing $L_{\min}$ (i.e., 10, 20, and 30). After the MP construction step, the imagery was classified by SVM using LIBSVM library [24]. In this study, 5% of the samples for each class from the ground truth data were randomly chosen as training samples, and the remaining samples compose the test set. The optimal parameters C and γ were chosen by fivefold cross-validation: $C = 32\,768$ and $\gamma = 0.0078125$. The resulting SVM classification map is given in Fig. 4(c), where the class *road* is shown in black while the class *nonroad* is shown in white. As seen from Fig. 4(c), road features were satisfactorily extracted by spectral–spatial classification. However, due to the spectral similarity, some areas (e.g., parks and buildings) are falsely classified as roads, which necessitates further processing.

As the road is a continuous feature, roads should be located in homogeneous areas. After spectral–spatial classification, the local homogeneity of gray values was then computed. First, the local Geary's C of each band was computed. The final local Geary's C result obtained by (3) is shown in Fig. 4(d). The result shows that the homogeneous areas have low intensity while edge pixels have large intensity. The thresholding algorithm with the intensity threshold obtained by (5) generates the result in Fig. 4(e). From Fig. 4(e), it is seen that the imagery was thresholded into two classes: *homogeneous* areas and *edge* pixels. The classification result and the thresholding result were then combined by applying the information fusion rule to obtain the initial road map. The fusion result is shown in Fig. 4(f). From Fig. 4(f), we can find that many man-made structures with spectral reflectance similar to that of roads are effectively discarded.

Finally, the initial road map was filtered by shape features to extract a pure road map. The filtering with the criteria that $T_{\text{Area}} = 50$, $T_{\text{LFI}} = 40$, and $T_{\text{ALJ}} = 50$ generates the result in Fig. 4(g). It is observed that most misclassified roads are eliminated by using shape features but several correct road segments were also removed. The removal of these roads is mainly because their completeness was damaged after the application of the fusion rule. The thinning result is shown in Fig. 4(h). The superposition result of the extracted road map and original remotely sensed imagery is shown together in Fig. 4(i).

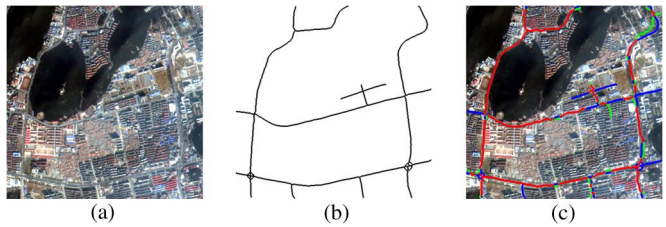

Fig. 5. (a) Image of the study area. (b) Road reference map. (c) Road extraction and original image superposition result.

TABLE II
QUANTITATIVE EVALUATION OF THE PROPOSED METHOD

Experiment	*Completeness*	*Correctness*	*Quality*
1	0.87	0.81	0.72
2	0.71	0.84	0.62

Fig. 5 shows road extraction results using a Ziyuan-3 satellite image of an inner city in Quanshan District, Xuzhou City. The test area in Fig. 5(a) has a spatial dimension of 469×477 pixels. The road reference map is presented in Fig. 5(b). In this experiment, the optimal parameters of SVM chosen by fivefold cross-validation are $C = 128$ and $\gamma = 0.5$. The thresholds for shape features were $T_{\text{Area}} = 60$, $T_{\text{LFI}} = 15$, and $T_{\text{ALJ}} = 50$. The road extraction and original image superposition result is shown in Fig. 5(c), where true positives, false positives, and false negatives are shown in red, green, and blue, respectively.

The quantitative evaluation results of the two experiments are given in Table II. From Table II, it is seen that the proposed method successfully distinguished main roads from urban remotely sensed imagery. However, Table II also shows that the completeness in studied area III is much lower than that in studied area II. This is mainly because the spatial pattern in studied area III is more complicated than that in study area II, and thus, more road segments are removed after filtering based on shape features.

The proposed method is also tested on an IKONOS imagery provided by Prof. H. Mayer. The studied area and the corresponding road reference map are given in Fig. 6(a) and (b), respectively. Fig. 6(c) shows the road centerline extraction result. The proposed method was quantitatively compared with those methods provided by Mayer *et al.* [25], and Table III presents the comparison results. As can be seen from the table, Bacher's and Hedman's methods obtain the highest *quality* value, i.e., 0.78, while 0.60 for the proposed method is moderate. Contrary to expectations, this study did not achieve the highest accuracy. The reason for this is that some misclassified segments are linear [see Fig. 6(c)] and cannot be filtered out using shape features. On the other hand, Fig. 6(c) also indicates that most misclassified roads are located in vegetation areas, and thus, in future investigations, it might be possible to improve the proposed method by integrating vegetation index.

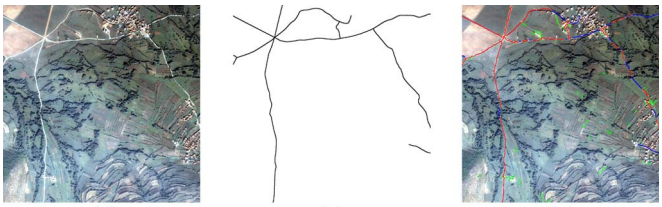

(a) (b) (c)

Fig. 6. (a) Image of the study area. (b) Road reference map. (c) Road extraction result with the parameters $T_{\mathrm{Area}} = 50$, $T_{\mathrm{LFI}} = 15$, and $T_{\mathrm{ALJ}} = 50$. The true positives are shown in red, false positives in green, and false negatives in blue.

TABLE III
COMPARISON OF DIFFERENT ROAD EXTRACTION METHODS

Author	*Completeness*	*Correctness*	*Quality*
Bacher	0.86	0.89	0.78
Gerke_W	0.75	0.52	0.44
Gerke_WB	0.71	0.84	0.63
Hedman	0.85	0.91	0.78
Malpica	0.6	0.89	0.56
Proposed	0.77	0.73	0.60

IV. CONCLUSION

An integrated main road extraction method has been proposed in this letter. The proposed method was tested using two experiments, and the following features are demonstrated: 1) The proposed method, based on the fusion of spectral–spatial classification and local spatial statistics, is feasible and effective for urban main road extraction and it was also confirmed that many man-made structures which have spectral reflectance similar to that of roads can be satisfactorily eliminated using the fusion scheme, and 2) shape features can retain linear features and most nonlinear features were removed. Filtering by shape features leads to an increase of road extraction accuracy.

The proposed method was tested on 4–6-m test images, and it worked well. However, if the image resolution is lower than 6 m, the local Geary's C cannot work correctly. This is because the road width at this resolution is only one to two pixels and the local homogeneity cannot be measured by local Geary's C. Hence, the proposed method is not suitable for low-resolution imagery. The thresholds of shape features were set by the trial and error method in this letter. To avoid the threshold selection problem and the limitation of only "main road" extraction, road shape features will be used as measures of structural information to extract roads in future research.

ACKNOWLEDGMENT

The authors would like to thank Prof. H. Talbot for providing the source code of path openings and closings, Prof. H. Mayer for providing the IKONOS data set, and E. Anson for polishing the language of this letter. The authors would also like to thank the editor and anonymous reviewers whose insightful suggestions have significantly improved this letter.

REFERENCES

[1] J. B. Mena, "State of the art on automatic road extraction for GIS update: A novel classification," *Pattern Recognit. Lett.*, vol. 24, no. 16, pp. 3037–3058, Dec. 2003.

[2] C. Poullis and S. You, "Delineation and geometric modeling of road networks," *ISPRS J. Photogramm. Remote Sens.*, vol. 65, no. 2, pp. 165–181, Mar. 2010.

[3] W. Z. Shi and C. Q. Zhu, "The line segment match method for extracting road network from high-resolution satellite images," *IEEE Trans. Geosci. Remote Sens.*, vol. 40, no. 2, pp. 511–514, Feb. 2002.

[4] M. J. Song and D. Civco, "Road extraction using SVM and image segmentation," *Photogramm. Eng. Remote Sens.*, vol. 70, no. 12, pp. 1365–1371, Dec. 2004.

[5] S. Das, T. T. Mirnalinee, and K. Varghese, "Use of salient features for the design of a multistage framework to extract roads from high-resolution multispectral satellite images," *IEEE Trans. Geosci. Remote Sens.*, vol. 49, no. 10, pp. 3906–3931, Oct. 2011.

[6] S. Hinz and A. Baumgartner, "Automatic extraction of urban road networks from multi-view aerial imagery," *ISPRS J. Photogramm. Remote Sens.*, vol. 58, no. 1/2, pp. 83–98, Jun. 2003.

[7] A. Plazaa, J. A. Benediktsson, J. W. Boardman, J. Brazile, L. Bruzzone, G. Camps-Valls, J. Chanussot, M. Fauvel, P. Gamba, A. Gualtieri, M. Marconcini, J. C. Tilton, and G. Trianni, "Recent advances in techniques for hyperspectral image processing," *Remote Sens. Environ.*, vol. 113, no. 1, pp. S110–S122, Sep. 2009.

[8] W. Su, J. Li, Y. H. Chen, Z. Liu, J. Zhang, T. M. Low, I. Suppiah, and S. A. M. Hashim, "Textural and local spatial statistics for the object-oriented classification of urban areas using high resolution imagery," *Int. J. Remote Sens.*, vol. 29, no. 11, pp. 3105–3117, Jun. 2008.

[9] C. W. Emerson, N. S. N. Lam, and D. A. Quattrochi, "A comparison of local variance, fractal dimension, and Moran's I as aids to multispectral image classification," *Int. J. Remote Sens.*, vol. 26, no. 8, pp. 1575–1588, Apr. 2005.

[10] Y. Tarabalka, J. A. Benediktsson, and J. Chanussot, "Spectral–spatial classification of hyperspectral imagery based on partitional clustering techniques," *IEEE Trans. Geosci. Remote Sens.*, vol. 47, no. 8, pp. 2973–2987, Aug. 2009.

[11] M. Fauvel, J. A. Benediktsson, J. Chanussot, and J. R. Sveinsson, "Spectral and spatial classification of hyperspectral data using SVMs and morphological profiles," *IEEE Trans. Geosci. Remote Sens.*, vol. 46, no. 11, pp. 3804–3814, Nov. 2008.

[12] D. Tuia, F. Pacifici, M. Kanevski, and W. J. Emery, "Classification of very high spatial resolution imagery using mathematical morphology and support vector machines," *IEEE Trans. Geosci. Remote Sens.*, vol. 47, no. 11, pp. 3866–3879, Nov. 2009.

[13] P. Gamba, F. Dell'Acqua, and G. Lisini, "Improving urban road extraction in high-resolution images exploiting directional filtering, perceptual grouping, and simple topological concepts," *IEEE Geosci. Remote Sens. Lett.*, vol. 3, no. 3, pp. 387–391, Jul. 2006.

[14] A. Grote, C. Heipke, and F. Rottensteiner, "Road network extraction in suburban areas," *Photogramm. Rec.*, vol. 27, no. 137, pp. 8–28, Mar. 2012.

[15] K. Price, "Urban street grid description and verification," in *Proc. 5th IEEE WACV*, 2000, pp. 148–154.

[16] M. Buckley and H. Talbot, "Flexible linear openings and closings," in *Mathematical Morphology and Its Applications to Image and Signal Processing*, vol. 18, G. Goutsias, L. Vincent, D. S. Bloomberg, and G. Goutsias, Eds. New York: Springer, 2000, ser. Computational Imaging and Vision, pp. 109–118.

[17] H. Heijmans, M. Buckley, and H. Talbot, "Path openings and closings," *J. Math. Imaging Vis.*, vol. 22, no. 2/3, pp. 107–119, May 2005.

[18] S. Valero, J. Chanussot, J. A. Benediktsson, H. Talbot, and B. Waske, "Advanced directional mathematical morphology for the detection of the road network in very high resolution remote sensing images," *Pattern Recognit. Lett.*, vol. 31, no. 10, pp. 1120–1127, Jul. 2010.

[19] C. Cortes and V. Vapnik, "Support-vector networks," *Mach. Learn.*, vol. 20, no. 3, pp. 273–297, Sep. 1995.

[20] L. Anselin, "Local Indicators of Spatial Association–LISA," *Geogr. Anal.*, vol. 27, no. 2, pp. 93–115, Apr. 1995.

[21] R. van Uitert and I. Bitter, "Subvoxel precise skeletons of volumetric data base on fast marching methods," *Med. Phys.*, vol. 34, no. 2, pp. 627–638, Feb. 2007.

[22] R. C. Gonzalez, R. E. Woods, and S. L. Eddins, *Digital Image Processing Using MATLAB*, 2nd ed. Knoxville, TN, USA: Gatesmark Publishing, 2009.

[23] C. Wiedemann, C. Heipke, and H. Mayer, "Empirical evaluation of automatically extracted road axes," in *Proc. CVPR*, 1998, pp. 172–187.

[24] C. Chang and C. Lin, LIBSVM—A Library for Support Vector Machines 2013. [Online]. Available: http://www.csie.ntu.edu.tw/~cjlin/libsvm

[25] H. Mayer, S. Hinz, U. Bacher, and E. Baltsavias, "A test of automatic road extraction approaches," *Int. Arch. Photogramm. Remote Sens. Spatial Inf. Sci.*, vol. 36, no. 3, pp. 09–214, 2006.